Vol. 10, No. 1, 2019
ISSN 2233-4203/ e-ISSN 2093-8950
INVITED ARTICLE www.msletters.org | Mass Spectrometry Letters

Comparison of Lipid Profiles in Head and Brain Samples of *Drosophila Melanogaster* Using Electrospray Ionization Mass Spectrometry (ESI-MS)

Hyun Jun Jang[1,2], Jeong Hyang Park[3], Ga Seul Lee[4], Sung Bae Lee[3], Jeong Hee Moon[4], Joon Sig Choi [2], Tae Geol Lee[1], and Sohee Yoon[1,*]

[1]*Center for Nano-Bio Measurement, Korea Research Institute of Standard and Science (KRISS), Daejeon 34113, Republic of Korea*
[2]*Department of Biochemistry, Chungnam National University, Daejeon 34134, Republic of Korea*
[3]*Department of Brain & Cognitive Sciences, DGIST, Daegu 42988, Republic of Korea*
[4]*Disease Target Structure Research Center, Korea Research Institute of Bioscience and Biotechnology (KRIBB), Daejeon 34141, Republic of Korea*

Received November 30, 2018; Revised December 19, 2018; Accepted December 19, 2018
First published on the web March 31, 2019; DOI: 10.5478/MSL.2019.10.1.11

Abstract : *Drosophila melanogaster* (fruits fly) is a representative model system widely used in biological studies because its brain function and basic cellular processes are similar to human beings. The whole head of the fly is often used to obtain the key function in brain-related diseases like degenerative brain diseases; however the biomolecular distribution of the head may be slightly different from that of a brain. Herein, lipid profiles of the head and dissected brain samples of *Drosophila* were studied using electrospray ionization-mass spectrometry (ESI-MS). According to the sample types, the detection of phospholipid ions was suppressed by triacylglycerol (TAG), or the specific phospholipid signals that are absent in the mass spectrum were measured. The lipid distribution was found to be different in the wild-type and the microRNA-14 deficiency model (miR-14Δ^1) with abnormal lipid metabolism. A few phospholipids were also profiled by comparison of the head and the brain in two fly model systems. The mass spectra showed that the phospholipid distributions in the miR-14Δ^1 model and the wild-type were different, and principal component analysis revealed a correlation between some phospholipids (phosphatidylethanolamine (PE), phosphatidylinositol (PI), and phosphatidylserine (PS)) in miR-14Δ^1. The overall results suggested that brain-related lipids should be profiled using fly samples after dissection for more accurate analysis.

Keywords : Lipid profile, *Drosophila* sampling, *Drosophila* brain, mass spectrometry (MS), electrospray ionization (ESI)

Introduction

Electrospray ionization-mass spectrometry (ESI-MS) is a technique for identification and structural analysis of analytes by ionizing a sample solution.[1-3] The sample solution is dispersed in the form of a fine spray of charged droplets, followed by solvent evaporation using a drying gas, and introduction of the gas-phase ions ejected from the highly charged droplets into a mass analyzer. Among various types of mass analyzers, quadrupole time-of-flight (QTOF) analyzer can perform tandem mass spectrometry (tandem MS, MS/MS) to identify molecular structures.[4-6] ESI-MS can be applied to most samples upon dissolution in a suitable solvent. It shows especially strong performance in the analysis of biological samples containing organic molecules like metabolites, lipids, proteins, DNAs, cyclopeptides, and amino acids, etc.[7-12]

Lipids are important components of cell membranes, act as messengers in intracellular signaling, and play an essential role in life support such as energy storage.[13] Lipids are classified according to their structures and functions. For instance, triacylglycerol (TAG), a glycerolipid that stores energy produced by its beta-oxidation, is composed of one glycerol and three fatty acid units.[14] Glycerophospholipid, composed of a hydrophilic phosphate head group and a hydrophobic fatty acid tail group, is a component of the thin lipid bilayer of the cell membrane. This lipid class includes phosphatidylcholine (PC), phosphatidyl ethanolamine (PE), phosphatidylserine (PS), phosphatidylinositol (PI), etc. The degradation products from TAGs and glycerol phospholipids are

*Reprint requests to Sohee Yoon
E-mail: shyoon@kriss.re.kr

involved in the cell signaling pathway.[11] Any disruption in the metabolism or concentration of these lipids leads to metabolic diseases like diabetes or degenerative brain diseases like Alzheimer's.[15,16]

In general, lipids of the same class have many different configurations depending on the degrees of unsaturation. Therefore, in lipidomics, lipid profiling is considered a key approach for comparing lipids between sample groups, and for obtaining identification of lipid species and relative quantitative information of hundreds of lipids in a single analysis.[17,18] ESI-tandem MS has been used to effectively perform lipid profiling of biological samples. Generally, lipid profiling involves lipid extraction from the biological sample, ion production by ESI, followed by identifying the lipid species and obtaining the degree of unsaturation and relative abundance information by MS or tandem MS.[19] Accurate preparation of samples containing lipids to be profiled is essential for responsible lipid profiling.

Being one of the most common model systems in biological studies, *Drosophila melanogaster* (fruits fly) is widely used for lipid metabolism in brain or energy metabolism studies that require statistical treatment because of its short life span and ability to cultivate large numbers of individuals in the laboratory.[20,21] It is also easy to express disease in *Drosophila* via genetic regulation.[22] Recently, the *Drosophila* model has been used to measure the lipid and neurotransmitter levels present in the brain.[23,24] In some research groups, the lipid profile of the *Drosophila* brain and metabolite distribution changes caused by drug treatment were measured by MS or MS imaging.[25,26] Preparing brain tissue samples of the fly for mass spectrometry is difficult because the length of the fly head is 8–900 μm and the height is 5–600 μm, while the brain is quite small (~500 μm in length and ~300 μm in height).[27] Therefore, the entire head of the fly is utilized in mass spectrometry[28-30] for the measurement of lipids, proteins, or metabolites in the brain tissue. In studies using MS imaging, the head sections of the control and disease cases were compared in terms of lipid distribution at depths of several nanometers from the tissue surface.[25-27] This approach has the advantage of obtaining accurate information of a single molecular layer from the tissue surface; however, a consecutive analysis of brain tissue sections by MS imaging is necessary to obtain the correlation with lipid distribution throughout the entire brain. However, consecutive sectioning of *Drosophila* head with thin tissue sections requires tremendous experimental skills. Therefore, lipid profiles of only the brain and the entire head were compared using extraction method.

In this study, we investigated the lipid species and distribution in *Drosophila* head and brain samples by ESI-QTOF MS, using the wild-type and microRNA-14 deficiency model (miR-14Δ^1) of *Drosophila melanogaster*. Since TAG is involved in phospholipid synthesis and regulation, all the cells store a small amount of the lipid.[31] Thus, microRNA-14 may cause lipid profile changes in the fly head, leading to an increased amount of TAG in the cell.[31] By comparative analysis of the lipid profiles of head and brain in each *Drosophila* sample, we could exactly confirm the difference in lipid information by mass spectrometry.

Experimental

Materials

Chloroform and ammonium acetate were purchased from Sigma Aldrich (St. Louis, USA), phosphate-buffered saline (PBS) from Life Technologies (CA, USA), and methanol and ethanol from Merck KGaA (Darmstadt, Germany). A pair of tweezers, used for dissection of fly heads, was purchased from Electron Microscopy Sciences (PA, USA).

Fly stock and sample preparation

The miR-14Δ^1 (stock number: 33067) and w1118 (wild-type; stock number 3605) models used in the experiment were obtained from Bloomington *Drosophila* Stock Center (BDSC; USA). *Drosophila* was cultured in dextrose/agar medium supplied by Biomax. (Seoul, Korea) at 25°C.

Lipids were extracted from 7-days-old wild-type (WT) flies using Folch lipid extraction method.[30] Figure 1 shows a schematic for lipid extraction from the *Drosophila* head and brain. Briefly, flies were put in a conical tube, frozen in liquid nitrogen, and shaken to separate the fly heads. The collected fly heads were put in a glass homogenizer, 0.5 mL of chloroform/ methanol (2:1, *v*/*v*) solvent was added, and homogenized for 15 min using a Teflon rod. The homogenates were transferred to an Eppendorf tube

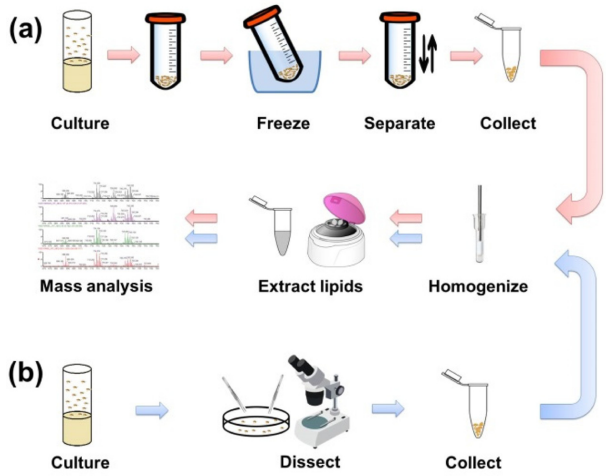

Figure 1. Workflow for lipid profiling of *Drosophila melanogaster* using mass spectrometry. Two types of samples of the microRNA-14 defect model and its wild-type-(a) head and (b) brain were used.

and centrifuged at 5000 g for 10 min at 4°C. After centrifugation, the supernatant was collected, and the extraction procedure was repeated with 500 μL of the extraction solvent used above. After mixing the two supernatants with 0.5 mL of 0.9% NaCl solution, the mixture was vortexed and centrifuged at 5000 g for 10 min at 4°C. The collected lower layer was dried under vacuum and stored in a deep freezer at -80°C before analysis. The dried lipid sample was dissolved in 1 mL of 5 mM ammonium acetate in chloroform/methanol (2:1, *v*/*v*) and the solution was vortexed and sonicated for 10 min.

Thirty-five fly heads were incubated for 1 min in ethanol and transferred to PBS solution for manual dissection to separate the brain and the outer peel. After dissection, the separated brains, and outer peels were collected to an eppendorf tube (Figure 1), and lipids were extracted in same manner as described above. Each fly sample was prepared in three sets of WT and miR-14Δ[1] to obtain reproducible measurements

Mass spectrometry

Mass spectrometry was performed in positive and negative ion modes on an ESI-QTOF mass spectrometer (Synapt™, Waters, MA, USA). The sample solution was sprayed at a flow rate of 0.5 μL/min through a fused silica capillary (I.D. 75 μm and O.D. 360 μm). The source temperature was 90°C. The spray voltages were 3.2 and 2.8 kV in positive and negative ion modes, respectively. The sampling and extraction cone voltages were 35.0 and 4.0 V, respectively. The cone gas flow rate was 50.0 L/h, the micro-channel plate voltage was 1.7 kV, and the trap collision energy was 6 eV. Tandem MS was performed under the following conditions: capillary voltage of 4.0 kV, sampling cone voltage of 25.0 V, and collision energy of 30–40 eV. Other conditions were the same as those given above. Mass spectra were recorded over the *m*/*z* range from 350 to 2000 Da with a 1.0 s scan time and a 0.02 s interscan delay. Three sets of fly samples were employed and the acquisition was repeated three times for each measurement. Assignments of lipid classification and compound structures were done based on references[23,32] and the mass spectrometry analysis tools of LIPID MAPS® Lipidomics Gateway (http://www.lipidmaps.org/resources/tools/index.php).

Data analysis

ESI-MS data were acquired by MassLynx 4.1 (Waters, MA, USA). Principal component analysis (PCA) was performed using a program of the self-written script for MATLAB (MathWorks, Inc., MA, USA). Three mass spectra were obtained from each of the four samples (WT head, WT brain, miR-14Δ[1] head, miR-14Δ[1] brain) and were subjected to PCA. All the spectra covering a range of *m*/*z* 680–880 were included in statistical analysis. The spectrum was normalized to the sum of the selected intensities and was mean-centered.

Results and discussion

Lipid distribution in *Drosophila* head and brain

We performed lipid profiling of the WT and the miR-14Δ[1] models to observe the difference in lipid distribution between the head of *Drosophila melanogaster* and its brain alone. The miR-14Δ[1] model is a genetically modified model with abnormalities in fat metabolism.[29] Figure 2 shows the mass spectra obtained in positive ion mode for lipids extracted from the head and the brain. In both cases, the distribution of TAGs extracted from the head was presented dominantly, with strong ion signals from *m*/*z* 680 to 860, and a small amount of PC was detected. Figure 2(a) and 2(c) show that the lipid distributions were almost similar in the heads of WT and miR-14Δ[1]. Most of the TAGs were detected in the form of the ammonium adduct ion, $[M+NH_4]^+$, because ammonium acetate was used to enhance ion production in ESI-MS.

In contrast to the head, only small amounts of TAG were observed in the mass spectra of the brain sample, while the mainly detected lipid was PC (Figure 2(b) and 2(d)). Interestingly, the relative distributions of PC peaks in the spectrum for the brain were different in WT and miR-14Δ[1]. The strongest PC ion in the WT brain (Figure 2(b)) was PC(32:2), whereas PC(34:2) was most intense ion observed in the miR-14Δ[1] brain (Figure 2(d)), which was about 3 times more intense than that of the WT brain case. Furthermore, intensities of TAG peaks at *m*/*z* 790 or higher for the miR-14Δ[1] model were measured to be ~50% lower than those of the WT case. Despite the large amounts of PC in the fly brain, detection of PC was suppressed compared to TAG in the head samples.

Unlike the positive ion mode, only phospholipid was recorded in the mass spectrum acquired in the negative ion mode (Figure 3). PE, PS, and PI, which advantageously form molecular ions in the negative ion mode, were detected in both head and brain samples of WT and miR-14Δ[1] types. Comparison of the mass spectra of WT head and WT brain, shown in Figure 3(a) and 3(b), reveal that the detected phospholipids were similar but their relative ratios were different. The relative intensity of PE(34:2) in WT brain was significantly lower than that in WT head, whereas PE(36:2e) and PE(36:2) increased. Particularly, the relative ratios among PE(34:2), PE(36:2e), and PE(36:2) were very different in the mass spectra for WT head and WT brain. The lipid ion signals measured from *m*/*z* 795 to 815 have very low intensities compared to other lipid peaks for WT head, and are difficult to detect with significant peaks when performing lipid profiling. On the other hand, these peaks can be observed during lipid profiling due to the relative increase in signal intensity. Moreover, the lipid peaks at *m*/*z* 810 and *m*/*z* 824 (not assigned) are difficult to find in the WT head spectrum, but can be seen clearly in the WT brain spectrum (Figure 3(b)). Comparison of the WT mass spectra indicate that

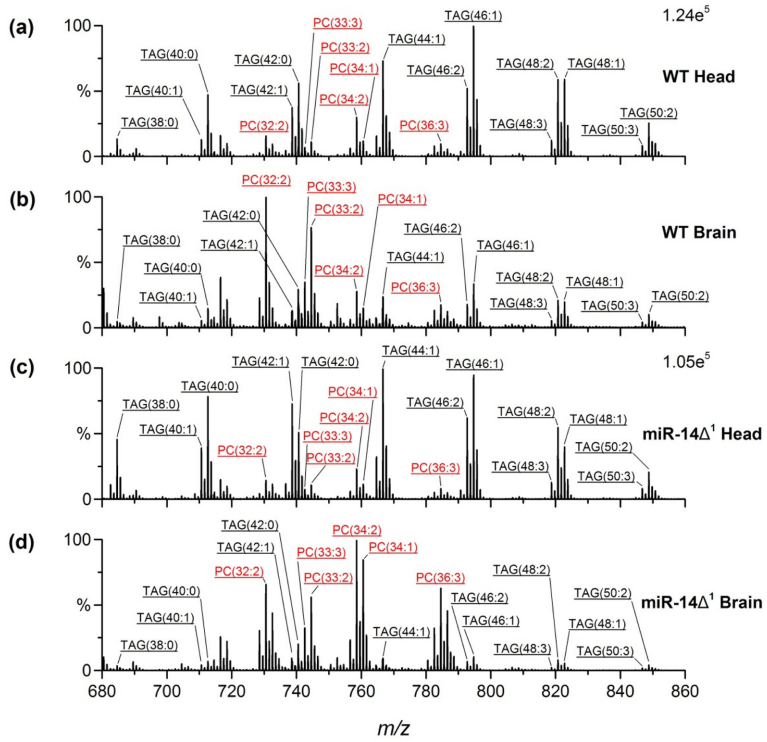

Figure 2. Positive-ion-mode mass spectra obtained by ESI-QTOF-MS. Lipids were extracted from (a) WT head, (b) WT brain, (c) miR-14Δ^1 head, and (d) miR-14Δ^1 brain. TAG ions were detected as $[M+NH_4]^+$ and PC ions as $[M+H]^+$.

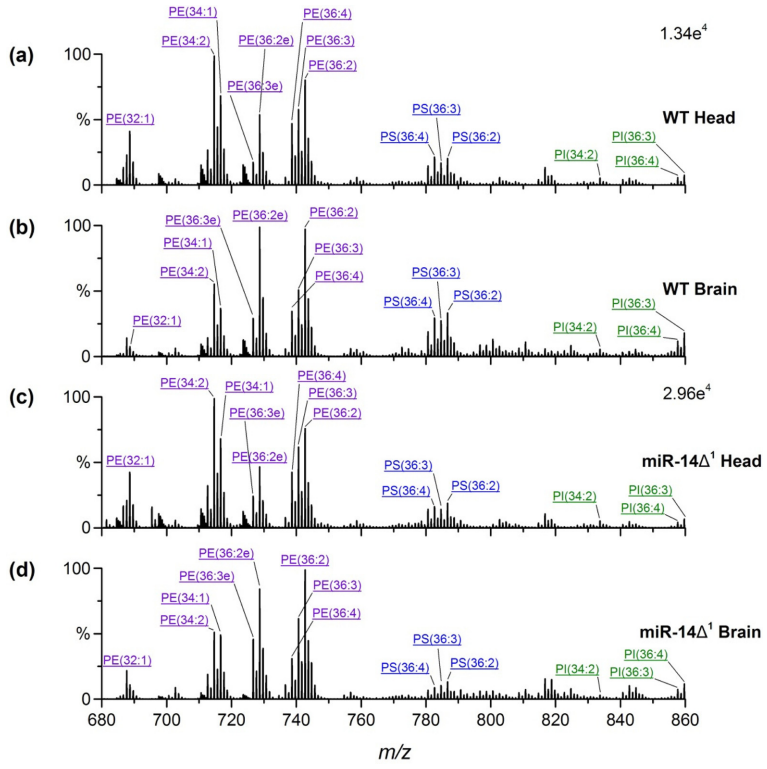

Figure 3. Negative-ion-mode mass spectra obtained by ESI-QTOF-MS. Lipids were extracted from (a) WT head, (b) WT brain, (c) miR-14Δ^1 head, and (d) miR-14Δ^1 brain.

phospholipid species extracted from the head and the brain were similar and that lipid detection is not inhibited by specific lipid peaks. The relative intensities of the negatively charged phospholipids between head and brain mass spectra are different because the lipids present in the outer peel are included in the head spectrum (data not shown). Thus, the dissection process is required to observe changes in lipids in the brain. For the miR-14Δ^1 model, the change patterns in the relative intensity of PE between head and brain mass spectra and in clarity of the lipid peaks at *m/z* 810 and *m/z* 824 (not assigned) were almost similar to those of the WT cases (Figure 3(c) and 3(d)). Comparison of the lipid spectra extracted from WT brain and miR-14Δ^1 brain (Figure 3(b) and 3(d), respectively) showed that the relative intensity distributions of PE were almost similar, but the distribution of PS and PI, lipids measured at *m/z* > 770, were slightly different.

An MS/MS analysis was performed to confirm the identities of lipid ions of interest. Figure 4 shows the MS/MS spectra of *m/z* 758.6 and *m/z* 782.5. In Figure 4(a), the ions at *m/z* 184 and at *m/z* 86 correspond to the PC head group and the choline head group, respectively, which are characteristic fragments of the protonated PC molecule. Thus, the MS/MS result confirmed the assignment of the precursor ion at *m/z* 758.6 as PC(34:2). In Figure 4(b), the MS/MS spectrum of the ion at *m/z* 782.5 indicates that the precursor is PS(36:4). The *m/z* 279 fragment ion is a fatty acid ion formed by side chain cleavage of PS(36:4). The peak at *m/z* 415 is formed by the neutral loss of one fatty acid side chain and serine from the precursor ion. Also, the loss of acyl side chain as ketene and serine produces a fragment ion at *m/z* 433. The loss of serine is the characteristic fragmentation in MS/MS of PS molecules, where *m/z* 695 corresponds to this loss in PS(36:4). The structure identification of other lipids were performed by MS/MS analysis.

Comparing the mass spectra of each case, we can identify what lipid is detected in positive and negative ion modes, and can obtain the relative increase or decrease in lipids in the head and brain samples and the relative changes in lipid signal intensity. However, it is necessary to confirm more precisely by statistical analysis which factors induce the most different results in mass spectrometry analysis.

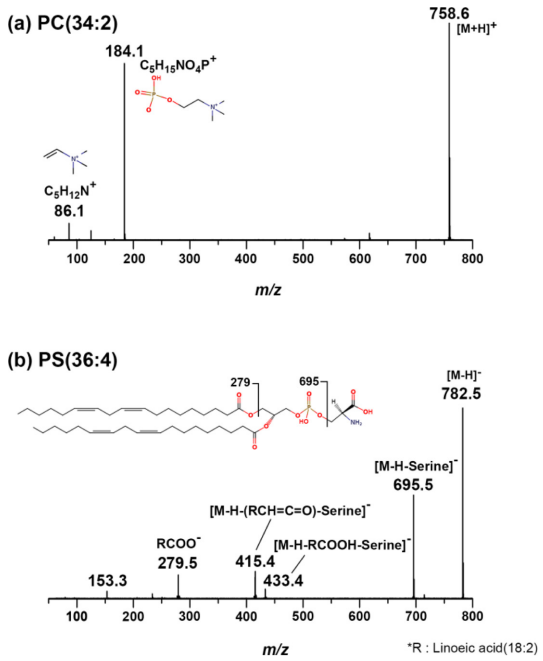

Figure 4. MS/MS spectra of (a) PC(34:2) at *m/z* 758.6 and (b) PS(36:4) at 782.5 measured in positive ion and negative ion modes, respectively.

Statistical analysis

Statistical analysis using PCA was performed to investigate the differences between lipid profiling of *Drosophila* head and brain samples, and to identify the significant lipids in the WT and miR-14Δ^1 models. The raw data obtained from the WT head, WT brain, miR-14Δ^1 head, and miR-14Δ^1 brain samples were subjected to PCA. Figure 5 shows the statistical results of the score plots and loading plots in each ion acquisition mode.

PCA score plots showed that head or brain sampling in *Drosophila* affects mass spectrometry for lipid profiling and that the lipidomic difference between brain samples is more significant than that between head samples in WT and miR-14Δ^1. As described in the positive-ion-mode mass spectrum (Figure 2), TAG and PC were the dominant molecules in WT/miR-14Δ^1 head and brain samples, respectively. These results were reflected in the loading plot of positive ion mode, as shown in Figure 5(a)- PC(32:2, 33:3, 34:2, 34:1, 36:3) and TAG(40:0, 42:1, 44:1, 46:1, 48:2, 48:1) ion peaks with high contribution to the PCA score plot were identified. Negative ion mode analysis revealed that PE(32:1, 34:2, 34:1, 36:3e, 36:2e, 36:4), PS(36:4, 36:3, 36:2), and PI(36:4, 36:3) made significant contribution to the difference between each sample, as shown in Figure 5(b). Lipid peaks with a loading plot score of 0.15 or higher and 0.01 or higher in the positive and negative ion modes, respectively, were extracted; the normalized relative intensities are shown in a bar graph for each of WT head, WT brain, miR-14Δ^1 head, and miR-14Δ^1 brain samples (Figure 5(c)). Opposite distributions of TAG and PC were obtained in the head and brain samples of both WT and miR-14Δ^1. The TAG ion signal had large intensities in both head samples and the decrease in intensity for brain samples was greater in the miR-14Δ^1 case. PC(32:2) and PC(33:3) showed the largest increase in signal intensity in WT brain.

In negative ion mode, some phospholipids showed significant differences between WT and miR-14Δ^1. In the miR-14Δ^1 brain sample, the levels of PE(34:1) and PE(36:3e) exceeded those in the WT brain by ~30% and

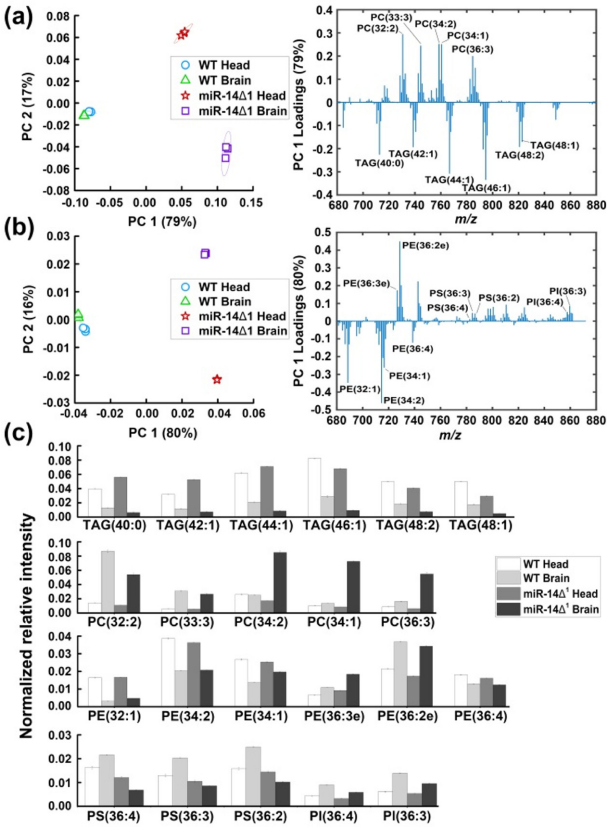

Figure 5. PCA results and relative quantification of lipid changes in head and brain samples of *Drosophila*. PCA score plot and loading plot in (a) positive and (b) negative ion modes. (c) Graphs of normalized relative intensity of lipids with loading scores of 0.15 or higher and 0.01 or higher in the positive and negative ion modes, respectively.

~40%, respectively. However, these lipid peaks differ slightly between the head samples of two *Drosophila* models, making it difficult to identify them as meaningful lipids for the miR14 defective disease. PS(36:4), PS(36:3), and PS(36:2) showed large changes in levels between WT and miR-14Δ^1 brain samples (Figure 5(c)). PS extracted from head samples was slightly reduced for miR-14Δ^1 compared to WT, but three PS levels were reduced to less than half for the brain samples. This significant lipid decrement is induced by miR-14Δ^1. PI(36:4) and PI(36:3) also showed changes in miR-14Δ^1 brain samples.

Lipid profiling in *Drosophila* brain using mass spectrometry is meaningful, but there are difficulties such as very small size and easy loss of part of the brain when dissecting the brain from the head. As an alternative, one may consider utilizing the entire fly head. However, it has been confirmed that excess TAG, existing outside the brain, inhibits the measurement of phospholipids and that relative signal intensity pattern of lipids appeared differently in the mass spectrum.

Conclusions

To compare the lipid profiles using *Drosophila melanogaster* samples, we have employed mass spectrometry of lipids extracted from the head and brain of wild-type and microRNA-14 defective model flies. According to the sample types, the detection of phospholipid signal, which plays important roles in brain function, was suppressed by TAG, or specific phospholipid signals, which are absent in the mass spectrum, were measured. In addition, the distribution of PE, PI, and PS in the miR-14Δ^1 model was determined in comparison with the WT brain sample. This study showed that profiling of brain-related lipids should be performed using samples after dissection for more accurate analysis.

Acknowledgments

This research was supported by the Development of Platform Technology for Innovative Medical Measurements Program (No. KRISS-2018-GP2018-0018), funded by Korea Research Institute of Standards and Science, and the Nano Material Technology Development Program (No. 2014M3A7B6020163) of the National Research Foundation (NRF), funded by the Ministry of Science, ICT & Future Planning.

References

1. Gaskell, S. J. *J. Mass Spectrom*. **1997**, 32, 677.
2. Wilm, M. *Proteomics*. **2011**, 10, M111.009407.
3. Banerjee, S.; Mazumdar, S. *Int. J. Anal. Chem.* **2012**, 2012, 1.
4. Glish, G. L.; Goeringer, D. E. *Anal. Chem*. **1984**, 56, 2291.
5. Chernushevich, I. V.; Loboda, A. V.; Thomson, B. A. *J. Mass Spectrom.* **2001**, 36, 849.
6. Van Den Heuvel, R. H. H.; Van Duijn, E.; Mazon, H.; Synowsky, S. A.; Lorenzen, K.; Versluis, C.; Brouns, S. J. J.; Langridge, D.; Van Der Oost, J.; Hoyes, J.; Heck, A. J. R. *Anal. Chem.* **2006**, 78, 7473.
7. Draper, J.; Lloyd, A. J.; Goodacre, R.; Beckmann, M. *Metabolomics*. **2013**, 9, 4.
8. Loo, J. A. *Mass Spectrom. Rev.* **1997**, 16, 1.
9. Han, X.; Gross, R. W. *Mass Spectrom. Rev.* **2005**, 24, 367.
10. Beck, J. L.; Colgrave, M. L.; Ralph, S. F.; Shei, M. M. *Mass Spectrom. Rev.* **2001**, 20, 61.
11. Kang, K. B.; Jang, D. S.; Kim, J.; Sung, S. H. *Mass Spectrom. Lett.* **2016**, 7, 45.
12. Lee, J.; Lee, S.; Kim, B.; Lee, J.; Kim, O. S.; Cha, E. *Mass Spectrom. Lett.* **2018**, 9, 30.
13. Van Meer, G.; Voelker, D. R.; Feigenson, G. W. *Nat. Rev. Mol. Cell Biol.* **2008**, 9, 1124.
14. Athenstaedt, K.; Daum, G. *Cell. Mol. Life Sci*. **2006**, 63, 1355.

15. Gilbert, L. I. *Mol. Cell. Endocrinol.* **2008**, 293, 25.
16. Kosicek, M.; Hecimovic, S. *Int. J. Mol. Sci*. **2013**, 14, 1310.
17. Shevchenko, A.; Simons, K. *Nat. Rev. Mol. Cell Biol*. **2010**, 11, 593.
18. Carvalho, M.; Sampaio, J. L.; Palm, W.; Brankatschk, M.; Eaton, S.; Shevchenko, A. *Mol. Syst. Biol*. **2012**, 8, 1.
19. Li, L.; Han, J.; Wang, Z.; Liu, J.; Wei, J.; Xiong, S.; Zhao, Z. *Int. J. Mol. Sci*. **2014**, 15, 10492.
20. McGurk, L.; Berson, A.; Bonini, N. M. *Genetics*. **2015**, 201, 377.
21. Baker, K. D.; Thummel, C. S. *Cell Metab*. **2007**, 6, 257.
22. Bilen, J.; Bonini, N. M. *Annu. Rev. Genet*. **2005**, 39, 153.
23. Kliman, M.; Vijayakrishnan, N.; Wang, L.; Tapp, J. T.; Broadie, K.; McLean, J. A. *Mol. Biosyst*. **2010**, 6, 958.
24. Phan, N. T. N.; Hanrieder, J.; Berglund, E. C.; Ewing, A. G. *Anal. Chem*. **2013**, 85, 8448.
25. Phan, N. T. N.; Fletcher, J. S.; Ewing, A. G. *Anal. Chem*. **2015**, 87, 4063.
26. Philipsen, M. H.; Phan, N. N. T.; Fletcher, J. S.; Malmberg, P.; Ewing, A. G. *ACS Chem. Neurosci.* **2018**, 9, 6, 1462.
27. Le, M. U. T.; Son, J. G.; Shon, H. K.; Park, J. H.; Lee, S. B.; Lee, T. G. *Biointerphases*. **2018**, 13, 03B414.
28. Nuwal, T.; Heo, S.; Lubec, G.; Buchner, E. *J Proteome Res*. **2011**, 10, 541.
29. Jeffries, K. A.; Dempsey, D. R.; Behari, A. L.; Anderson, R. L.; Merkler, D. J. *FEBS Lett*. **2014**, 588, 1596.
30. Singh, V.; Sharma, R. K.; Athilingam, T.; Sinha, P.; Sinha, N.; Thakur, A. K. *J. Proteome Res.* **2017**, 16, 3863.
31. Xu, P.; Vernooy, S. Y.; Guo, M.; Hay, B. A.; *Curr. Biol.* **2003**, 13, 790.
32. Hammad, L. A.; Cooper, B. S.; Fisher, N. P.; Montooth, K. L.; Karty, J. A. *Rapid Commun. Mass Spectrom*. **2011**, 25, 2959.